

On the mechanism of carbon nanostructures formation at reaction of organic compounds at high pressure and temperature

Nataliya P. Satonkina, and Dmitry A. Medvedev

Citation: *AIP Advances* **7**, 085101 (2017); doi: 10.1063/1.4990710

View online: <http://dx.doi.org/10.1063/1.4990710>

View Table of Contents: <http://aip.scitation.org/toc/adv/7/8>

Published by the [American Institute of Physics](#)

Articles you may be interested in

[Effects of a static inhomogeneous magnetic field acting on a laser-produced carbon plasma plume](#)

AIP Advances **7**, 085002 (2017); 10.1063/1.4995527

[Temperature dependence of the non-local spin Seebeck effect in YIG/Pt nanostructures](#)

AIP Advances **7**, 085102 (2017); 10.1063/1.4986848

[Multi-tests for pore structure characterization-A case study using lamprophyre](#)

AIP Advances **7**, 085204 (2017); 10.1063/1.4997749

[A selection rule for transitions in PT-symmetric quantum theory](#)

AIP Advances **7**, 085001 (2017); 10.1063/1.4991032

[A novel in situ electrochemical NMR cell with a palisade gold film electrode](#)

AIP Advances **7**, 085205 (2017); 10.1063/1.4997887

[Rabi-like splitting from large area plasmonic microcavity](#)

AIP Advances **7**, 085201 (2017); 10.1063/1.4996715

HAVE YOU HEARD?

Employers hiring scientists and
engineers trust

PHYSICS TODAY | JOBS

www.physicstoday.org/jobs



On the mechanism of carbon nanostructures formation at reaction of organic compounds at high pressure and temperature

Nataliya P. Satonkina^{1,2,a} and Dmitry A. Medvedev^{1,2}

¹*Lavrentyev Institute of Hydrodynamics, Novosibirsk 630090, Russia*

²*Novosibirsk State University, Novosibirsk 630090, Russia*

(Received 16 June 2017; accepted 24 July 2017; published online 2 August 2017)

Based on the analysis of the data on the behavior of electric conductivity at the detonation of condensed high explosives (HEs) with the composition $C_aH_bN_cO_d$ and the carbon mass fraction higher than 0.1, the conclusion was made of the presence of long carbon nanostructures. These structures penetrate all the space of reacting HE. The structures are formed already in the chemical peak region, and they evolve along the detonation wave. © 2017 Author(s). All article content, except where otherwise noted, is licensed under a Creative Commons Attribution (CC BY) license (<http://creativecommons.org/licenses/by/4.0/>). [<http://dx.doi.org/10.1063/1.4990710>]

I. INTRODUCTION

Condensed carbon of different modifications is released at the detonation of high explosives with the composition $C_aH_bN_cO_d$ and negative oxygen balance. Ultrafine diamonds were found in conserved detonation products (DP).^{1,2} Despite the serious age of this discovery, there still remain several questions which provoke intense discussion. There is no common opinion about the shape of carbon particles at the carbon condensation during the detonation, about the condensation proceeding, and about the moment of formation of single particles.

In the literature, there are different viewpoints on the geometry of carbon inclusions. Results obtained by different investigation methods lead to different conclusions. In the work,³ carbon condensation to single particles was simulated with further formation of fractal structures from these particles. The mechanism restricting the growth of single particles was proposed. In the work,⁴ extended structures were obtained in a numerical experiment on the condensation of carbon. When the mass fraction of carbon is higher than 0.1, the stage of single particles is absent, and the condensation produces directly the extended structures. The electric conductivity of these structures was calculated which agrees well with the experimental data.

The viewpoint of the existence of single particles is shared by many authors (see for example⁵⁻¹⁰). In the work,⁵ a dynamic model of carbon condensation at the detonation of trinitrotoluene (TNT) was proposed based on the results of the electric conductivity investigation. The author of work⁶ considered the energy release at the condensation and obtained the growth of single carbon particles during several microseconds. In the work⁹ on the behavior of the electric conductivity at the detonation of triaminotrinitrobenzene (TATB), the growth of carbon particles in the Taylor wave was considered supposing the thermal electric conductivity mechanism.

There are several works where the data obtained using the synchrotron radiation are interpreted as an existence and growth of single carbon particles to the size of several tens of micrometers during several microseconds (for example, work¹¹). On the contrary, it was found in the work¹² using the same method that at the detonation of hexanitrostilbene $C_{14}H_6N_6O_{12}$, single particles appeared faster than in 0.5 microseconds, and the particle size of 2.7 nm remained constant during the whole measurement time (3 microseconds).

^aElectronic mail: snp@hydro.nsc.ru.

Thus, different investigation methods reveal both the extended structures which are hard to detect by the small angle x-ray scattering, and single particles found in conserved detonation products. The model of carbon condensation at the detonation is absent.

High pressure and temperature at the detonation of condensed HEs restrict the circle of experimental investigation methods, and the interpretation of the data obtained is ambiguous. At the present stage, comparison of the available experimental data is the most effective method. Under the assumption of a connection of electric properties and the presence of carbon,^{13,14} the data on electric conductivity is the ultimate source of information.

TNT has the highest amount of carbon among all HEs, the carbon mass fraction in molecule is 0.37, and the fraction of free carbon in the CJ point is 0.27.¹⁵ Further we will discuss that the electric conductivity in TNT can be satisfactorily explained by carbon nets.

For other HEs such as TATB, RDX (cyclotrimethylene-trinitramine), HMX (cyclotetramethylene-tetranitramine), and PETN (pentaerythritol tetranitrate), the relation between carbon and conductivity was not considered until recently due to relatively small amount of condensed carbon. It was proposed in works^{13,14} to explain the maximum value of conductivity by the formation of carbon structures in the chemical peak. Hence, it was supposed that carbon is fully condensed before the CJ point, and free carbon in detonation products is the remnant after the end of chemical reaction. In the framework of this model, the uniform dependence was obtained for the maximum conductivity and the conductivity in the CJ point for five HEs.

Thus, the condensation of carbon is inseparably connected to the electric conductivity. In this paper, we discuss the most realistic hypotheses of conductivity at the detonation of condensed HEs. It is shown that only the contact mechanism can explain the experimental data. HEs with the mass fraction of carbon higher than 0.1 are considered (TNT, RDX, TATB).

II. EXPERIMENTAL DATA ON THE BEHAVIOR OF ELECTRIC CONDUCTIVITY AT THE HE DETONATION

The detonation wave consists of the shock front, the adjacent chemical peak, and the Taylor rarefaction wave which is separated from the chemical peak by the Chapman – Jouguet (CJ) plane.

Typical electric conductivity profile is shown in Fig. 1. There is a fast growth to the maximum value, then a decrease with a gradient dependent on the explosive type, and after the inflection point, a slow variation in the Taylor wave with a small value. Maximum conductivity σ_{max} corresponds to a region inside the chemical peak. The inflection point σ_{CJ} at the $\sigma(t)$ graph is related to the CJ point.^{13,14} The Zeldovich-von Neumann-Döring theory assumes that at the CJ point, chemical reactions are completed. Thus, in Fig. 1, the chemical reaction takes place at $0 < t < 0.05$ microseconds.

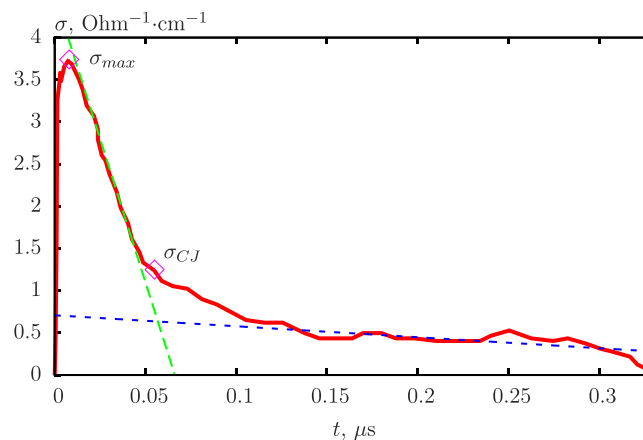


FIG. 1. Graph of conductivity at the detonation of RDX.

TABLE I. Data on electrical conductivity, critical diameter, thermodynamic and mechanical characteristics of TATB, RDX, TNT.

N	HE	ρ , g/cm ³	T_{CJ} , K	P_{CJ} , kbar	r_{CJ}	σ_{CJ} , Ohm ⁻¹ cm ⁻¹	r_c	σ_{max} , Ohm ⁻¹ cm ⁻¹	d_{cr} , mm
1	TATB	1.8	2762	267	0.208	10.0	0.279	19.1	6.35 ¹⁶ ($\rho \approx 1.7$)
2	TNT	1.0	3398	71	0.128	8.9		15.0	3÷5 ¹⁷ ($\rho \approx 1.51$)
3	TNT	1.6	3434	191	0.260	26.8	0.370	~100	16 ¹⁸ ($\rho = 1.62$)
4	RDX	1.2	3964	148	0.030	0.4		1.8	2 ÷ 4 ¹⁷ ($\rho \approx 1$)
5	RDX	1.6	3675	252	0.066	1.25	0.162	4.2	

Despite the absence of a complete conductivity theory, it is possible using the experimental data to exclude conductivity mechanisms which are not decisive for the electric properties of the detonation wave, and to make some conclusions about the geometry of carbon inclusions.

In the Table I, the data for HEs based on TATB, TNT, and RDX are presented. The notation is following: ρ is the initial density, T_{CJ} , P_{CJ} and r_{CJ} are temperature, pressure and the mass fraction of condensed carbon in the CJ point, r_c is the carbon fraction in molecule, σ_{CJ} and σ_{max} is the conductivity in the CJ point and the maximum conductivity, correspondingly, d_{cr} is the critical diameter from works.^{16–18} Temperature, pressure and mass fraction of condensed carbon in the CJ point were obtained numerically in work.¹⁵

All the HEs chosen are well known and intensely investigated. They have drastically different characteristics such as sensitivity, temperature and pressure in the detonation wave. The parameters of the detonation wave for HMX are close to those of RDX and PETN.

Presently, the most popular viewpoint is that in HEs with a slightly negative oxygen balance (PETN, RDX, HMX), the conductivity in the chemical peak could be related to the chemoionization analogous to the process of combustion¹⁹ where free electrons with high mobility appear as a result of chemical reaction. In the work,¹⁷ besides the chemoionization, the ionization of intermediate detonation products (DP), the dissociation of PD, and the thermal emission from carbon particles are listed as a source of charge carriers. The conductivity both in the chemical peak and in the Taylor wave are explained by the thermal emission. The existence of a correlation between the conductivity σ at the CJ point and the amount of condensed carbon was shown in works.^{20,21} There exist also works where the value of σ_{CJ} is explained by the ionic conductivity²² and by the thermal ionization.⁹

Let us consider different conductivity mechanisms from the standpoint of the experimental data presented.

III. DISCUSSION

A. Chemoionization

It was established by the comparison of experimental data on the duration of the reaction zone and the region of high conductivity that the maximum value of conductivity σ_{max} is reached inside the reaction zone.^{19,22,23} Chemoionization is thought to be the most probable cause of conductivity in the chemical peak region. The concentration of charge carriers n due to chemoionization is by definition connected with the number of reacted molecules. For the densities lower than the critical one, the speed of decomposition is maximal in the shock front and then monotonically decreases.²⁴ Following the argument of chemoionization, conductivity should be the higher the faster the initial substance decomposes, that is the maximum of conductivity σ_{max} should be close to the detonation front. According to our data for HEs with well defined conductivity peak, σ_{max} is reached at about the half of duration of the zone of increased conductivity,^{4,19,22,25–27} i.e., far from the front which contradicts to the relation of the conductivity σ and the intensity of reactions.

On the other hand, the number of elementary chemical reactions per unit time increases with the decrease of the duration of the reaction zone, and, according to Hariton's principle, the duration of the reaction zone is proportional to the critical diameter. Overall speed of chemical decomposition in RDX is close to that in TNT (see Table I). The conductivity in TNT is however higher by an order of magnitude $\sigma_{maxTNT2} \approx 8\sigma_{maxRDX4}$. For TATB based HE, the conductivity has an intermediate value $\sigma_{maxTNT2} > \sigma_{maxTATB} > \sigma_{maxRDX4}$ whereas the critical diameter is larger. Thus, the data of Table I show the absence of the dependence of maximum conductivity on the critical diameter.

The time of existence of free electrons in the chemical peak can play a significant role. If electrons produced in chemoionization are immediately captured by atoms forming ions, they have no time to make a contribution into conductivity, and the conductivity would be an ionic one. The mobility of ions is however insufficient to produce experimentally observed conductivity.²⁸ In the case of a large time of existence of free electrons, the concentration of charge carriers and, hence, the conductivity would increase in the course of chemical reaction. In the detonation wave, pressure and density reach maximum values near the front and then decrease monotonically.^{17,24,29,30} When pressure and density decrease, the intensity of recombination decreases,³¹ the mobility of electrons increases, and the concentration of reacting component decreases. From this, one would expect that conductivity would at least not fall at the decrease of pressure and density which is not observed.

Hence, we can conclude that chemoionization does not explain the experimental data. There is no relation between the speed of chemical decomposition and the maximum value σ_{max} . The explanation of highly nonuniform conductivity distribution is also absent.

In the works,^{13,14} the correlation between the maximum value of conductivity σ_{max} and the carbon content in a molecule r_c was demonstrated based on experimental data for five HEs. The increase of the maximum value σ_{max} with the increase of the HE density with the same grain size was observed. We suppose that this fact is related to the increase of the density of carbon, and it is a crucial factor for the conductivity.

In our opinion, the conductivity inside the chemical peak region is provided by carbon nanostructures which are produced at the destruction of molecules displacing other atoms into the space between structures.^{32,33} The data of Table I show the dependence of the maximum conductivity σ_{max} on the mass fraction of carbon r_c , and the absence of relation with the critical diameter and the chemoionization.

B. Relation between electric conductivity and temperature

In many works, the conductivity at the detonation is related to the high temperature. Temperature is however the most badly defined among all detonation parameters. Results of both calculations and experiments give sometimes even qualitatively different behavior of $T(\rho)$. Nevertheless, it is commonly accepted that the temperature at the detonation of TNT is lower than one at the detonation of RDX, HMX, and PETN.

The relation between temperature and conductivity can be provided by thermal ionization and thermal emission. Thermal ionization is the appearance of charge carriers (free electrons and ions) due to the high temperature. Thermal emission is the emission of free electrons from the surface of carbon particles. The temperature dependence of the ionic conductivity is qualitatively the same as of the electronic one. In the case of the same concentration of ions and electrons, the electronic conductivity would dominate due to higher mobility of charge carriers. Hence, we consider here electrons as charge carriers.

The temperature dependence of the conductivity for both the thermal ionization and thermal emission is exponential $\sigma \sim n_e \sim \exp(-\frac{E}{kT})$ with the activation energy of order of several eV.³⁴ The multiplier dependent on pressure, concentration of carriers, etc. changes for different HEs only slightly.

It was obtained experimentally that for three of listed in Table I HEs, the conductivity increases with the increase of density.^{4,19,22,25-27} The behavior of temperature is more complex. Figure 2 shows the temperature in the CJ point for different density of HE.¹⁵ For RDX, HMX and PETN, temperature decreases slightly with the increase of density. For TNT, the dependence $T(\rho)$ is non-monotonous given the same values of T at different densities (Table I, TNT₂ and TNT₃). Since the mobility

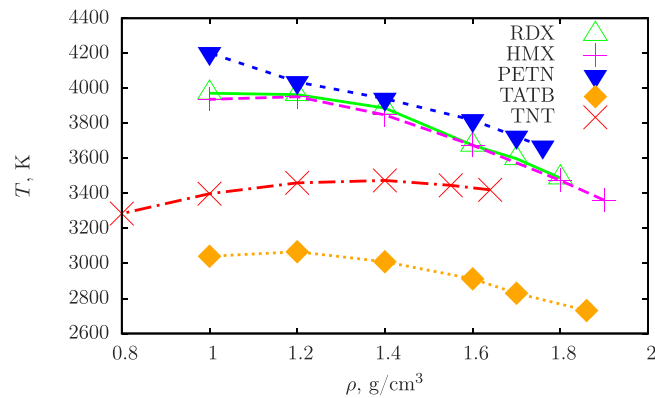


FIG. 2. Temperature at the CJ point, based on data from work.¹⁵

of electrons increases and recombination processes slows down at the decrease of pressure and density³¹ (in our case for TNT₂), it could be expected that σ_2 should be larger than σ_3 . Experiments give however that $\sigma_{CJ2}/\sigma_{CJ3} = 1/3$, $\sigma_{max2}/\sigma_{max3} \approx 1/6$, the values for smaller density are lower. This contradicts to the assumption of the thermal nature of conductivity.

The increase of conductivity with the increase of density can not be explained by temperature which is lower for RDX at higher density. This also supports the non-thermal origin of conductivity.

Besides, the temperature for RDX is higher than the one for TNT by ~ 450 K at significantly lower values of σ . For TATB based HE, the temperature is lower than the one for TNT by ~ 500 K which does not produce a strong exponential dependence in experimental data (Table I).

It was noticed earlier in work²⁸ that the estimate of the degree of thermal ionization by the Saha formula,³¹ i.e., the ratio of the number of ionized atoms to the total number of atoms gives the value of $\sim 10^{-6}$ which does not explain the experimental data on conductivity.

The thermal emission was investigated in detail in the work.²⁸ Following phenomena influencing the thermal emission were considered: the growth of carbon particles with time, the increase of the work function with the increasing size of a carbon particle, the decrease of the work function due to interaction with dense ambient products. The interaction of electron with surrounding positively charged carbon particles was also taken into account. It was obtained that the concentration of free electrons in the Taylor wave in TNT can be as high as 10^{19} cm^{-3} due to the thermal emission. This value is ten times lower than the one estimated from experimental value of conductivity $2 - 4 \text{ Ohm}^{-1} \text{ cm}^{-1}$. It was noted that the value obtained from experiments is close to the value estimated based on the thermal emission. It was impossible to make a choice between the thermal emission and the contact mechanism. In the works,^{20,22,35} maximum conductivity at the detonation of TNT was $100 - 250 \text{ Ohm}^{-1} \text{ cm}^{-1}$ which is two orders of magnitude higher than the value obtained in the work.²⁸ The values of conductivity in the work²⁸ were underestimated due to imperfect experimental method. Thus, necessary concentration of electrons should be 10^{22} cm^{-3} , and the thermal emission can not be a satisfactory explanation. Such a high concentration of electrons is not present at the detonation.

Hence, thermal ionization and thermal emission are certainly present in the detonation wave but they are not the determining factor for the conductivity. Table I shows that the increase of density and carbon fraction influence the conductivity more strongly than the value temperature.

C. Contact mechanism of electric conductivity

The relation of the conductivity with carbon can be considered using the carbon density, its volume and mass fraction. Each parameter has its advantages. The density gives the objective estimate of the amount of carbon, and it reflects most fully the influence of the conduction along carbon nets. The volume fraction was shown in the works^{4,40} to give an analytic relation under certain assumptions. The mass fraction is however always known, and it does not depend on the compression along the detonation wave.

In the works of Gilev,^{35,36} the maximum value of conductivity at the detonation of TNT was estimated from a percolation model. It was obtained that even the total amount of carbon is not sufficient to explain observed values, and highly conductive elongated structures need to exist already in the chemical peak region.

Let us estimate the conductivity of a cube with side 1 cm with a content of carbon equal to that in TNT of maximum density, i.e., $m_C = \rho_{max} \cdot V \cdot r_c = 1.6 \cdot 0.37 = 0.6 \text{ g}$ ($V = 1 \text{ cm}^3$). The conductivity of carbon varies in a broad range, from dielectric diamond to almost metallic one for highly-oriented graphite. Conductivity of graphite depends on the modification of the crystal lattice and on the crystallographic orientation, and it varies from ~ 244 to $1250 \text{ Ohm}^{-1}\text{cm}^{-1}$.^{37,38} The conductivity of highly-oriented graphite can be as large as $20000 \text{ Ohm}^{-1}\text{cm}^{-1}$.³⁹ The liquid state of carbon is possible at the detonation¹⁰ which has conductivity $\sim 1000 \text{ Ohm}^{-1}\text{cm}^{-1}$.³⁹ A carbon rod with a mass of 0.6 g and a length $l = 1 \text{ cm}$ with a conductivity of carbon $\sigma_C \approx 1000 \text{ Ohm}^{-1}\text{cm}^{-1}$ (work³⁴) has effective conductivity $\sigma \approx 240 \text{ Ohm}^{-1}\text{cm}^{-1}$ which is close to the experimental data. This value describes the process better than the estimates based on the thermal emission. These calculations support the hypothesis on a contact origin of conductivity at the detonation of condensed HEs with electric current along penetrating carbon nanostructures both in the chemical peak and in the Taylor wave.

1. Model of carbon condensation

To illustrate the model, consider the conductivity profile of Fig. 1. Before the arrival of the detonation front, HE is a dielectrics, and carbon is bounded in molecules. The increase of conductivity to maximum values σ_{max} corresponds to the destruction of HE molecules with simultaneous growth of carbon nets. The decrease of conductivity from σ_{max} to σ_{CJ} reflects the transition of carbon into a non-conductive phase which can be explained by oxidation reactions leading to thinning and partial destruction of conductive structures. Between 50 and 100 ns, the gradient of $\sigma(t)$ is lower which can be related to the lower speed of oxidation reactions due to the decrease of concentration of reactants. The region of $t > 0.1$ microsecond corresponds to the Taylor wave and single carbon particles. It follows from this model that σ_{max} and σ_{CJ} are the characteristics of the same structure at different moments of time, the change of conductivity reflects the evolution of carbon nets, and the aggregation of carbon atoms into structures of different scale occurs already in the reaction zone.

Thus, the condensed carbon considered in calculation is not released at the CJ point. On the contrary, this carbon is the remnant of structures formed in the region of chemical reaction.

2. Discussion

Molecular dynamics simulations show that the details on interparticle interaction do not influence significantly the time of coagulation. Aggregation of carbon atoms is determined by diffusion and proceeds in picoseconds.^{33,40} At thermodynamic parameters characteristic for the detonation, the state of carbon corresponds to the condensed phase,^{7,10} in contrast to other substances (N, N₂, H₂O, H, O, CO, CO₂, etc.). Probability of aggregation at a collision of two carbon atoms is close to 100%, whereas reactions of gaseous substances under the detonation conditions require of order of 1000 collisions for one elementary reaction.²⁹

In the works,^{4,40} it was obtained that at the carbon mass fraction higher than 0.1, the coagulation of carbon proceeds immediately to branched nanostructures and not to single particles with further formation of fractals as supposed in the work.³ The already present in an HE molecule united carbon atoms will enhance this process (for example, benzene ring in TNT or cross-like structure in PETN).

Following works confirm the fast aggregation of carbon atoms. Authors of the works^{32,33,41,42} assert that the aggregation of carbon occurs already in the reaction zone. V. F. Anisichkin obtained in work⁴¹ that carbon components of molecules of fine-grained mixture HEs completely mix before the oxidation, i.e., inside the reaction zone, and the oxidation occurs later. O.N. Breusov demonstrated from energy considerations³² that the formation of carbon clusters is related to the partial breakup of chemical bonds in molecules and to the formation and growth of carbon skeleton. In the work,³³ the clustering of carbon at the heating of molecules of TATB, HMX and PETN was simulated by

the molecular dynamics. Carbon nanostructures in the reaction zone were obtained. Filamentary structures of the diameter of 10–40 nm found in conserved detonation products^{43,44} can be the remnants of fractal structures formed at condensation in the region of chemical peak.

Carbon is able to condense in elongated structures with fractional dimension. Foam-like structures were obtained in inert atmosphere at low pressure.^{45,46} In the work,⁴⁷ formation of nets with a dimension 2.2 was observed, the formation of carbon clusters at combustion and detonation of gas mixtures was investigated, and clusters of different modifications we obtained, from fullerene-like to long branched carbon structures.

Below a certain fraction of carbon, the formation of penetrating structures becomes impossible due to the lack of sufficient amount of conductive substance. In the works,^{4,40} the threshold volume fraction of carbon at which the formation of connected nets in DP is possible was obtained in numerical experiments to be about 0.07. Carbon however influence the conductivity even at the fraction lower than 0.07.^{13,14} In such case, the existence of another carbon-related conductivity mechanism is possible, for example, highly-conductive carbon inclusions in a medium with low conductivity. When the carbon fraction and the contact conductivity decrease, the role of the ionic mechanism increases.

In an extreme case of the detonation of gas mixtures, a great progress in understanding the electric properties was made. In the work,⁴⁸ the conductivity model due to thermal ionization was considered, the improved by considering quantum-mechanical effects model of work²⁸ was proposed, and a good agreement with experimental data was obtained. The model used is based on the presence of free electrons in detonation products. The formula applied was derived under assumption of rare collisions which is valid for gas detonation but not applicable for condensed HEs with three orders of magnitude higher density. Despite the external similarity of the detonation process in gases and in condensed HEs, the nature of electric properties of these media is different, and the values of conductivity differ by three orders of magnitude.

Let's summarize. Under extreme conditions, carbon in organic compounds tends to aggregate in elongated structures. Atoms of nitrogen, oxygen and hydrogen chemically bound with carbon are present at the surface of such structures.⁴⁹

With the present state of investigation technology, it is impossible to directly observe elongated carbon structures during the detonation process directly due to the very short duration of the process and the aggressive media. The later factor hinders the revealing of such structures since they get thinned and broken in a chemically active media. Only conserved detonation products are available for investigation which provide only an overall information. Thus, the analysis of the electric properties measured at the detonation process seems to be a very promising and so far an ultimate investigation method.

The results of the present work are useful not only for the study of detonation and kinetics of HEs. The investigation of the behavior of media under extreme conditions characteristic for the explosion is rather restricted in methods, and the explosion becomes an ultimate approach. The results are useful for the fast developing interdisciplinary science, the abiogenesis⁵⁰ (formation of organic compounds at the early stage of the origin of life at young Earth, abiogenic formation of organic molecules characteristic for living organisms). Under high pressure and temperature, the formation of carbon chains and hydrocarbons occurs. The skeleton of all organic molecules is made of carbon-carbon bonds. Since carbon is one of the indispensable components of the living matter, the condition of explosion can model the conditions of meteoritic impacts, planetary depths, volcanos. Hence, the work was useful for astrobiology⁵¹ and geochemistry.

IV. CONCLUSION

Experimental data on the electric conductivity are used as the diagnostic tool and the indicator of the state of organic compounds under high pressure and temperature. The consideration of the most realistic hypotheses of conductivity shows that only the contact mechanism can explain high conductivity values obtained in experiments. This leads to the conclusion of existence of spatial carbon structures which form a connected nets. Such nets penetrate all the volume of reacting media and enable the flow of electric current when voltage is applied. Chemical reactions lead to the thinning

and disruption of the structures producing individual carbon formations which are found in conserved detonation products.

ACKNOWLEDGMENTS

The work was supported by RFBR, Grant N 15-03-01039.

- ¹ A. I. Lyamkin *et al.*, Dokl. Akad. Nauk. **33**, 705 (1988).
- ² N. R. Creiner, D. S. Phillips, J. D. Johnson, and F. Volk, *Nature* **333**, 440 (1988).
- ³ A. P. Ershov and A. L. Kupershtokh, *Combust. Explos. Shock Wave*. **27**(2), 111 (1991).
- ⁴ N. P. Satonkina, A. P. Ershov, E. R. Prueel, and D. I. Karpov, in *Proceeding XXIX Int. Conf. Physics of Extreme States of Matter*. (2014).
- ⁵ P. I. Zubkov, *J. Eng. Thermophys.-Russ* **24**(1), 57 (2015).
- ⁶ S. Bastea, *Appl. Phys. Lett.* **100**, 214106 (2012).
- ⁷ J. A. Viecelli, S. Bastea, J. N. Glosli, and F. H. Ree, *J. Chem. Phys.* **115**, 2730 (2001).
- ⁸ S. Bastea, *Scient. Rep* **7**, 42151 (2012).
- ⁹ M. M. Gorshkov *et al.*, *Combust. Explos. Shock Wave* **43**(1), 78 (2007).
- ¹⁰ V. V. Danilenko, *Combust. Explos. Shock Wave* **41**, 577 (2005).
- ¹¹ K. A. Ten, E. R. Prueel, and V. M. Titov, *Fullerenes, Nanotubes, Carbon Nanostr.* **20**, 587 (2012).
- ¹² M. Bagge-Hansen *et al.*, *J. Appl. Phys.* **117**, 245902 (2015).
- ¹³ N. P. Satonkina, *J. Appl. Phys.* **118**, 245901 (2015).
- ¹⁴ N. P. Satonkina, *Combust. Explos. Shock Wave* **52**, 488 (2016).
- ¹⁵ K. Tanaka, *Detonation Properties of Condensed Explosives Computed Using the Kihara-Hikita-Tanaka Equation of State* (National Chemical Laboratory for Industry, Tsukuba Research Center, 1983).
- ¹⁶ B. M. Dobratz and P. C. Crawford, *LLNL Explosives Handbook Properties of Chemical Explosives and Explosive Simulants LLNL University of California*, Livermore, California – (UCRL – 52997, 1985).
- ¹⁷ L. P. Orlenko, (Ed.), *Explosion Physics [Fizika vzryva]*, I. M.: Fizmatlit, 2002. (in Russian).
- ¹⁸ A. N. Dremin, S. D. Savrov, and K. K. Trofomov, *Detonation waves in condensed matters [Detonatsionnye volny v kondensirovannykh sredakh]* (Nauka, Moscow, 1970).
- ¹⁹ A. P. Ershov, N. P. Satonkina, and G. M. Ivanov, *Russ. J. Phys. Chem. B* **26**(12), 21 (2007).
- ²⁰ B. Hayes, in *Proceeding 4th Symposium on Detonation*. White Oak, ACR-126, 1965. P. 595.
- ²¹ S. D. Gilev and A. M. Trubachev, *Techn. Phys. Russ. J. Appl. Phys.* **46**(9), 1185 (2001).
- ²² A. P. Ershov and N. P. Satonkina, *Combust. Explos. Shock Wave* **45**, 205 (2009).
- ²³ N. P. Satonkina, *arXiv:1603.08069* [physics.chem-ph]. 2016.
- ²⁴ B. G. Loboiko and S. N. Lubyatinsky, *Combust. Explos. Shock Wave* **36**, 716 (2000).
- ²⁵ A. P. Ershov, N. P. Satonkina, and G. M. Ivanov, *Techn. Phys. Lett.* **30**, 1048 (2004).
- ²⁶ A. P. Ershov and N. P. Satonkina, *Combust. Flame* **157**, 1022 (2010).
- ²⁷ N. P. Satonkina and A. A. Safonov, *J. Eng. Thermophys.-Russ* **18**(2), 177 (2009).
- ²⁸ A. P. Ershov, *Fiz. Goren. Vzryva* **11**(6), 798 (1975) (in Russian).
- ²⁹ Ya. B. Zeldovich, *Zh. Eksp. Teor. Fiz.* **10**(5), 542 (1940) (in Russian).
- ³⁰ A. V. Fedorov *et al.*, *Combust. Explos. Shock Wave* **48**, 302 (2012).
- ³¹ Ya. B. Zeldovich and Yu. P. Raizer, *Physics of Shock Waves and High-Temperature Hydrodynamic Phenomena [Fizika udarnykh voln i gidrodinamicheskikh yavlenii]*. M., Fizmatgiz, 1963, 632 p.
- ³² O. N. Breusov, *Russ. J. Phys. Chem. B* **21**(11), 110 (2002).
- ³³ Y. Wen, C. Zhang, X. Xue, and X. Long, *Phys. Chem. Chem. Phys.* **17**, 12013 (2015).
- ³⁴ I. K. Kikoin, *Spravochnik* (Atomizdat, Moscow, 1976).
- ³⁵ S. D. Gilev and A. M. Trubachev, in *Proceeding 12th International Symposium on Detonation*. San Diego, CA, 2002. ONR333-05-2. P. 240.
- ³⁶ S. D. Gilev, Doctoral dissertation, Lavrentyev Institute of Hydrodynamics SB RAS, Novosibirsk, Russia, 2009.
- ³⁷ Kh. Kuhlning, *Handbook of physics [Spravochnik po fizike]* (Mir, Moscow, 1982).
- ³⁸ R. L. Powell and G. E. Childs, *American Institute of Physics Handbook* (Mir, Moscow, 1972).
- ³⁹ V. N. Korobenko, A. I. Savvatimskiy, and R. Cheret, *Int. J. Thermophys.* **20**(4), 1247 (1999).
- ⁴⁰ N. P. Satonkina, E. R. Prueel, and D. I. Karpov, in *Proceeding XV Int. Detonation Symposium*. 2014.
- ⁴¹ V. F. Anisichkin, *Combust. Explos. Shock Wave* **43**, 580 (2007).
- ⁴² V. F. Anisichkin, *Rus. J. Phys. Chem. B* **35**(6), 30 (2016).
- ⁴³ D. L. Ornellas, *Calorimetric Determinations of the Heat and Products of Detonation for Explosives: October 1961 to April 1982 NASA STI/Recon Technical Report N. April 1982*. 3.
- ⁴⁴ Y. Nomura and R. Kawamura, *Carbon* **22**(2), 189 (1984).
- ⁴⁵ A. V. Rode *et al.*, *Appl. Phys. A: Mat. Science. Proc.* **69**, S755 (1999).
- ⁴⁶ A. Zani, D. Dellasega, V. Russo, and M. Passoni, *Carbon* **56**(May), 358 (2013).
- ⁴⁷ A. A. Vasil'ev and A. V. Pinaev, *Combust. Explos. Shock Wave* **44**, 317 (2008).
- ⁴⁸ X. Wang, D. Ye, and F. Gu, *Combust. Explos. Shock Wave* **44**, 101 (2008).
- ⁴⁹ A. Krüger, F. Kataoka *et al.*, *Carbon* **43**, 1722 (2005).
- ⁵⁰ A. V. Emeline, V. A. Otroshchenko *et al.*, *J. Photochem. Photobiol. C: Photochem. Rev.* **3**, 203 (2003).
- ⁵¹ A. A. Novoselov *et al.*, *Astrobiol.* **13**, 294 (2003).